Gas Chromatography Mass Spectroscopic, Spectral, Structural and Quantum Mechanical Studies of Behenic Acid

K. Gomathi[1], R. Rathikha[2], and P. Rajesh[3]

[1]Research Scholar, PG and Research Department of Physics, Presidency College Chennai 600005, Tamilnadu, India.

[2]Assistant Professor, PG and Research Department of Physics, Presidency College Chennai 600005, Tamilnadu, India.

[3]Assistant Professor, Department of Physics, School of Basic Sciences Vels Institute of Science Technology and Advance Studies Pallavaram, Chennai 600 117, Tamilnadu, India.

Abstract – The behenic acid has been synthesising from methanol extract of the leaves of *Aegle marmelos*. The experimental and predicted theoretical like Fourier-transform infrared spectroscopy spectrum have excellent correlation. Density functional theory have performed by using B3LYP/6-311G++(d,p) level is employed for obtaining the electronic, spectroscopic, inter-molecular interaction and natural bond orbital properties of title compound. The ultraviolet–visible spectroscopy spectroscopic studies along with highest occupied molecular orbital and lowest unoccupied molecular orbital analysis were used to elucidate information regarding charge transfer within the molecule. The frontier molecular orbitals, and global reactivity descriptors have been calculated and interpreted. Electron acceptor and donor region are shown in the molecular electrostatic potential; Mulliken population analysis on atomic charges is also calculated and additionally conformed in molecular docking studies.

INTRODUCTION

India is widely known as the botanical garden of the world since it is the largest producer of medicinal herbs [1]. Medicinal plants act as an indigenous source of new compounds possessing therapeutic value and can also be used in drug development. Eighty percentage of the population of developing countries depend on traditional medicines, mostly natural plant products, for their primary health care needs as estimated by WHO [2]. Because of the growing recognition of natural products the demand for medicinal plants has been increasing all over the world. They have minimal toxicity, are cost effective and pharmacologically active, and provide an easy remedy for many human ailments as compared to the synthetic drugs which are a subject of adulteration and side effects [3]. The alarming increase in the rate of infection by antibiotic-resistant microorganisms has urged scientists to search for compounds which have potential antimicrobial activity [4]. The ability to synthesize compounds by secondary metabolism possessing antimicrobial potential makes plants an invaluable source of pharmaceutical and therapeutic products [5]. The effectiveness of plant extracts on microorganism has been studied worldwide [6]–[9].

Bael (*Aegle marmelos*) has been known to be one of the most important medicinal plants of India since Charak (1500 B.C.) [10]. More than 100 phytochemical compounds have been isolated from various parts of the plant, namely phenols, flavonoids, alkaloids, cardiac glycosides, saponins, terpenoids, steroids, and tannins. These compounds are well known to possess biological and pharmacological activity against various chronic diseases such as cancer and cardiovascular and gastrointestinal disorders [11]–[13]. Antioxidant, antiulcer, antidiabetic, anticancer, antihyperlipidaemic, antiinflammatory, antimicrobial, antispermatogenic effects have also been reported on various animal models by the crude extracts of this plant [14]–[22]. Every part of *Aegle marmelos* plant such as its fruits, stem, bark, and leaves possesses medicinal property and is used for treating

various eye and skin infections [23]. Leaf is considered to be one of the highest accumulatory parts of the plant containing bioactive compounds which are synthesized as secondary metabolites [24]. The present study was, therefore, aimed at evaluating the phytochemical behenic acid from *Aegle marmelos* aqueous and methanolic leaf extracts using gas chromatography mass spectroscopic (GC-MS) technique.

Behenic acid is a carboxylic acid, the saturated fatty acid with formula $C_{23}H_{46}O_2$. In appearance, it consists of white to cream color crystals or powder with a melting point of 80°C and boiling point of 306°C. Commercially, behenic acid is often used to give hair conditioners and moisturizers their smoothing properties. It is also used in lubricating oils, and as a solvent evaporation retarder in paint removers. Its amide is used as an antifoaming agent in detergents, floor polishes and dripless candles. Reduction of behenic acid yields behenyl alcohol. Pracaxi oil (from the seeds of *Pentaclethra macroloba*) is a natural product with one of the highest concentrations of behenic acid, and is used in hair conditioners.

In addition, these calculation methods widely contribute to the spectroscopic studies performed experimentally. Density functional theory (DFT) has been intensively employed for the calculation of various properties of some thiophene derivatives such as molecular structure, ultraviolet–visible (UV-vis) sepctra, Fourier-transform infrared (FT-IR) spectra, HOMO–LUMO energies and charge distributions behaviors. The vibrational frequencies were analyzed by means of potential energy distribution (PED) calculation by using vibrational energy distribution analysis (VEDA 4) program. Frontier molecular orbital (FMO) studies were carried out for the behenic acid.

Extraction of Phytochemical Behenic Acid From the Leaves of *Aegele marmelos* Using Gas Chromatography Mass Spectroscopic Technique

Extraction of oil from *Aegle marmelos* leaves was carried out by Soxhlet extraction method. Leaves of *Aegle marmelos* leaves were collected and cut into small pieces and air dried for several days. The dried leaves were then pulverized with a local kitchen blender. Exactly 100 g of the pulverized leaves were macerated in 500 ml of methanol for 7 days in air tight clean flat bottomed container at room temperature with occasional shaking and stirring. The extract was then filtered first through a fresh cotton plug and then with a Whatman filters paper. The filtrate was combined and concentrated using a rotary evaporator at low temperature (40°C) and pressure. GC-MS plays a key role in the analysis of known and unknown components of the plant origin. GC-MS ionizes compound and measures their mass numbers. The use of mass spectrometry (MS) in most cases coupled to an appropriate separation technique as gas chromatography. The identified phytochemical behenic acid is then subjected to experimental and theoretical quantum chemical calculations to identify the property of the title molecule.

Materials and Methods

The behenic acid was purchased from Sigma–Aldrich Chemical Company (USA) with a stated purity of greater than 99% and it was used as such without further purification. The FT-IR spectra were recorded using a Shimadzu FTIR-8700 spectrometer in the mid-IR range of 400–4000 cm^{-1}.

Computational Details of Behenic Acid

The optimized molecular geometry and vibrational frequencies of behenic acid was carried out using the Gaussian 03W software package [25] using DFT-B3LYP combined with the 6-311++G(d,p) basis set to characterize all stationary points as minima. The vibrational band assignments of normal modes of vibration are made on the basis of PED calculated by using the VEDA 4 program. The molecular electrostatic potential (MEP), HOMO–LUMO energy gap, thermodynamic properties at different temperature were calculated by DFT method.

The optimized structure of behenic acid is shown in Figure 1. The most optimized structural bond length, bond angle, dihedral angle have been analyzed by B3LYP/6-311++G(d,p) basis set and is given in Table I. From the calculated values, we can find that most of the optimized bond length and bond angles are slightly varied than the experimental values of structurally related molecules. In the present case, the bond lengths C_{20}–C_{21} (1.5141), C_4–C_5 (1.5138), C_5–C_6, C_6–C_7 (1.5137) has been calculated using DFT analysis. The optimized calculated bond lengths C_{20}–C_{21} (1.5141) are larger and C_{25}–H_{71} (1.1165) are shorter. Further the strong bond is found to be C_{20}–C_{21} (1.5141) and smaller value of bond length weak bond C_{25}–H_{70}, C_{25}–H_{71} (1.1165). This decrease in bond length may be due to the fact that the electronegativity of oxygen atom with neighbouring atoms. In spite of the differences, the calculated geometries represent a good approximation and they are the bases for calculating vibrational frequencies and thermodynamical properties.

VIBRATIONAL ANALYSIS OF BEHENIC ACID

FT-IR spectra of behenic acid was obtained using 6-311++G(d,p) basis set by DFT method. Theoretical and experimental FT-IR spectra are shown in Figure 2 and the vibrational band assignments are given in Table II.

I. C–H Vibrations

The linear aliphatic organic compound shows the presence of C–H stretching vibrations in the region 3100–3000 cm^{-1}. Calculated aromatic C–H stretching vibrations coincide exactly with the experimental value showing at 3100 cm^{-1} for behenic acid. The carbon–hydrogen in-plane bending vibrations usually occur as a strong to weak intensity band in the region 1300–1000 cm^{-1}. In the present case, the in-plane bending vibrations were identified at 1310, 1287 cm^{-1}. All the vibrations were observed within the expected ranges which are affected by the functional group vibrations.
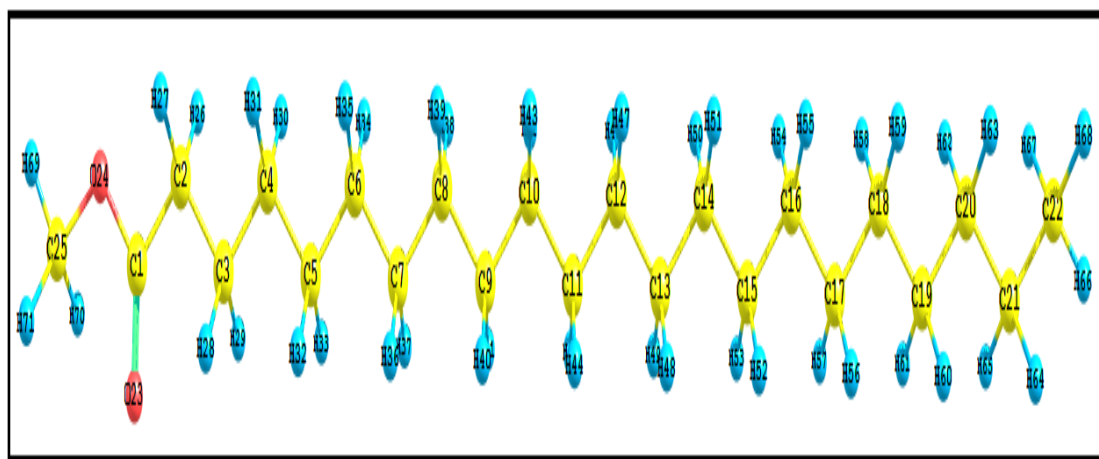

FIGURE 1

OPTIMIZED STRUCTURE OF BEHENIC ACID

The C–H out-of-plane bending vibrations normally appeared in the region 1000–730 cm^{-1}. In this case, the C–H out–of–plane bending vibrations are found at 1015, 970, 916 cm^{-1}.

II. C–O, C=O and O–H Group Vibrations

The vibrational bands of the terminal carboxylic groups of behenic acid includes the C–O, C=O and O–H vibrational modes. Behenic acid has a strong band due to the C=O stretching vibrations. Carboxyl group are usually observed in the region at 1750–1700 cm^{-1} in which the position of C=O stretching band depends on the physical state, mass and electronic effects, intra- and intermolecular hydrogen bonding and another strong band at 1650–1400 cm^{-1} due to the stretching of the C–O band. According to the literature, a very strong band has appeared in IR spectrum at 1715 cm^{-1} confirming the C=O stretching band vibrations. It is initiated at the top end of the C=O stretching region of the spectra due to the enormous force constant (21.2 m dyne) of the bond. The other three bands with very strong to medium intensity at 1527 cm^{-1} is designated as C–O stretching vibrations. If the bond lengths are different, the related force constants are also different. The in-plane bending vibrations are observed at 863 cm^{-1} and out-of-plane bending vibrations are found at 364 cm^{-1}. The position of the band due to the C–O stretching vibrations is dependent in the nature of both the acidic and the alcoholic compounds, although the latter is less important. The entire bending vibrations are much by sub sequentially interaction with the chain. The carbonyl group is the most important in the IR spectrum because of its strong intensity of absorption and high sensitivity towards minor changes in its environment.

TABLE I

OPTIMIZED GEOMETRICAL PARAMETERS OF BEHENIC ACID

Bond Length	B3LYP/6-31G(d, p)	Bond Length	B3LYP/6-31G(d, p)
C_1–C_2	1.4956	C_{12}–H_{47}	1.1221
C_1–O_{23}	1.2321	C_{13}–C_{14}	1.5136
C_1–O_{24}	1.3708	C_{13}–H_{48}	1.1221
C_2–C_3	1.5133	C_{13}–H_{49}	1.1221
C_2–H_{26}	1.1228	C_{14}–C_{15}	1.5136
C_2–H_{27}	1.1228	C_{14}–H_{50}	1.1221
C_3–C_4	1.5134	C_{14}–H_{51}	1.1221
C_3–H_{28}	1.1221	C_{15}–C_{16}	1.5136
C_3–H_{29}	1.1221	C_{15}–H_{52}	1.1221
C_4–C_5	1.5138	C_{15}–H_{53}	1.1221
C_4–H_{30}	1.1221	C_{16}–C_{17}	1.5136
C_4–H_{31}	1.1221	C_{16}–H_{54}	1.1221
C_5–C_6	1.5137	C_{16}–H_{55}	1.1221
C_5–H_{32}	1.1221	C_{17}–C_{18}	1.5136
C_5–H_{33}	1.1221	C_{17}–H_{56}	1.1221
C_6–C_7	1.5137	C_{17}–H_{57}	1.1221
C_6–H_{34}	1.1221	C_{18}–C_{19}	1.5136
C_6–H_{35}	1.1221	C_{18}–H_{58}	1.1221
C_7–C_8	1.5136	C_{18}–H_{59}	1.1221
C_7–H_{36}	1.1221	C_{19}–C_{20}	1.5135
C_7–H_{37}	1.1221	C_{19}–H_{60}	1.1221
C_8–C_9	1.5136	C_{19}–H_{61}	1.1221
C_8–H_{38}	1.1221	C_{20}–C_{21}	1.5141

$C_{20}–H_{39}$	1.1221	$C_{20}–H_{62}$	1.1219
$C_9–C_{10}$	1.5136	$C_{20}–C_{63}$	1.1219
$C_9–H_{40}$	1.1221	$C_{21}–C_{22}$	1.5068
$C_9–H_{41}$	1.1221	$C_{21}–H_{64}$	1.1222
$C_{10}–C_{11}$	1.5136	$C_{21}–H_{65}$	1.1222
$C_{10}–H_{42}$	1.1221	$C_22–H_{66}$	1.1167
$C_{10}–H_{43}$	1.1221	$C_22–H_{67}$	1.1169
$C_{11}–C_{12}$	1.5136	$C_{22}–H_{68}$	1.1169
$C_{11}–H_{44}$	1.1221	$O_{24}–C_{25}$	1.4273
$C_{11}–H_{45}$	1.1221	$C_{25}–H_{69}$	1.1177
$C_{12}–C_{13}$	1.5136	$C_{25}–H_{70}$	1.1165
$C_{12}–H_{46}$	1.1221	$C_{25}–H_{71}$	1.1165

The properties of carbonyl group are directly tied to its electronic structure as well as geometric positioning. In both inter and intramolecular factors affect the carbonyl absorptions in frequent organic compounds due to the inductive effects, mesomeric effects and conjugation effects.

III. C–C Vibrations

The carbon–carbon stretching vibrations occur in the region 1625–1400 cm^{-1} [26],[27]. Here the frequencies are observed in the region 1431 cm^{-1} (IR) were assigned to C–C stretching vibration.
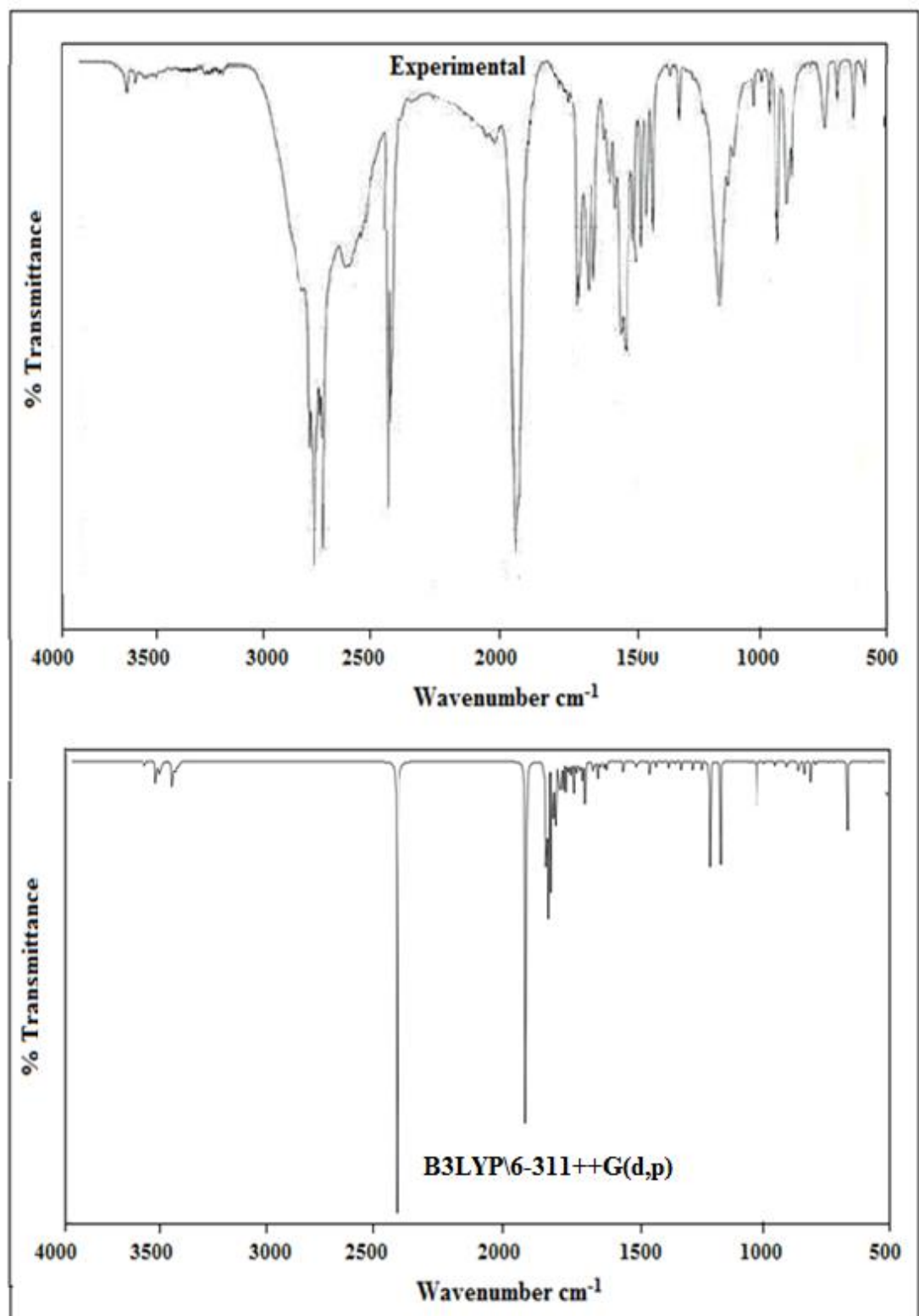
FIGURE 2

SIMULATED B3LYP/6-311++G(D,P) AND EXPERIMENTAL FT-IR OF BEHENIC ACID

DFT frequencies for C–C bonds in the ring show excellent agreement with the experimental data. The in-plane C–C–C deformation bands occur in the region at 651–509 cm^{-1} while the out-of-plane C–C–C deformation

bands occur in the region 477–282 cm^{-1} [18],[29]. The present frequencies observed in the region 340 cm^{-1} and 462 cm^{-1} belong to the in-plane and out-of-plane deformations, respectively.

TABLE II

VIBRATIONAL WAVE NUMBERS OBTAINED for BEHENIC ACID at DFT/6-311++G(d,p)

Calculated B3LYP/6-311++G(d,p)	Observed Frequencies FT-IR	Vibrational Assignments + (PED)
3157	3150	ν CH$_3$ (76)
3155	–	ν CH$_3$ (100)
3109	–	ν CH (98)
3108	3108	ν CH (100)
3106	–	ν CH (89)
3103	–	ν CH (91)
3101	3100	ν CH (93)
3098	–	ν CH (100)
3096	–	ν CH (34)
3093	–	ν CH (46)
3090	–	ν CH (28)
2999	–	ν CH (27)
2077	2062	ν OC (69)
1722	1715	ν OC (87)
1527	1531	δ HCH (42) + ν OC (13)
1461	–	δ HCH (42)
1459	1455	δ HCH (28)
1451	–	δ HCH (58)
1444	1442	δ HCH (19)
1439	–	δ HCH (66)
1434	1431	ν CC (42) + δ HCH (32)
1423	1423	δ HCH (24)
1414	–	δ HCH (33)
1411	1412	δ HCH (59)
1410	–	δ HCH (31)
1407	–	δ HCH (53)
1407	1400	δ HCH (51)
1404	–	δ HCH (68)
1404	–	δ HCH (46)
1397	1479	δ HCH (44)
1394	–	δ HCH (73)
1384	1386	δ HCC (26)
1379	–	δ CH$_3$ (23)
1367	1361	δ HCC (32)
1357	1348	δ HCC (28)
1353	–	δ CH$_3$ (36)
1342	1341	δ HCC (24)
1332	–	δ HCC (28)

1314	–	δ HCC (16)
1304	1310	δ HCC (23)
1294	1280	ν OC (76)
1285	1287	τ HCOC (63) + ν CH (17)
1270	–	δ HCC (16) + τ HCOC (42)
1258	–	δ HCC (41)
1205	–	δ HCC (18) + ν CC (28)
1198	–	δ HCC (68)
1178		ν CC (19) + δ HCC (21)
1056	1058	ν CC (18) + ν OC (47)
1048	–	ν CC (13)
1033	–	ν CC (47)
1015	1015	ν CC (36) + ν CH (18)
993	–	ν CC (28)
969	–	ν CC (43)
943	940	ν CC (56)
916	916	ν CC (33) + ν CH (11)
998	–	ν CC (88)
980	970	ν CC (62)
863	860	ν OC (52)
680	668	δ OCO (36)
746	–	τ HCCC (23) + ν CH (17)
694	698	δ CCC (52) γ OCOC (62)
509	–	δ CCC (53)
486	–	δ CCC (24)
462	453	δ CCC (16)
411	–	δ CCC (20)
364	–	δ COC (19)
340	–	τ CCCC (23)
308	–	δ COC (45)
287	–	δ COC (68)
235	–	δ CCC (21)
212	–	δ CCC (23)

HOMO–LUMO ANALYSIS

This also predicts the most reactive position in the π-electron system and various reactions involved in the conjugated systems. The HOMO shows various prominent donor orbitals and the LUMO shows that of prominent acceptor orbitals. The HOMO orbitals are represented by green colour and the LUMO orbitals are represented by red colour. The former represents negatively charged surfaces, i.e., electrophiles while the latter represents positively charged surfaces, i.e., nucleophiles. The HOMO–LUMO energy gap shows the charge transfer interaction taking place within the molecule. Higher energy of the HOMO (7.29243) indicates the electron donating ability of the inhibitor molecule to the unoccupied d-orbital of the metal and lower energy of the LUMO (−0.45933) indicates the electron accepting ability of the inhibitor molecule from the metal. Larger donor energy value implies that the inhibition efficiency of the inhibitor is less due to low reactivity with the metal surface and lower DE value implies that the inhibitor is having higher inhibition efficiency due to high reactivity with metal surface [30]. The electronegativity (3.87588) is an important quantum chemical parameter

which represents the distribution of electrons in the molecular structure and electron attracting capacity of the molecule, respectively. Global hardness (3.87588) and global softness (0.25800) are another important properties to measure the reactivity of an inhibitor. A hard molecule has a large energy gap while a soft molecule is characterized by a small energy gap. Soft molecules are more reactive than hard ones because they could easily offer electrons to an acceptor.

ELECTRONIC TRANSITIONS of BEHENIC ACID

The electronic spectra of behenic acid was compared with calculated spectra at DFT calculation using B3LYP/6-311++G(d,p) basis set as shown in Figure 3. The absorption wavelength (λ_{max}), the main assignment, oscillator strength (f), and excitation energies (E) of 6.219, 7.4601 and 7.6333 are shown in Table III. The observed spectra of the molecule have been studied and three intense peaks of 320, 120 and the observed band at 320 nm is due π(donor)–π^*(acceptor) transition.

TABLE III

UV–VIS EXCITATION ENERGY OF BEHENIC ACID

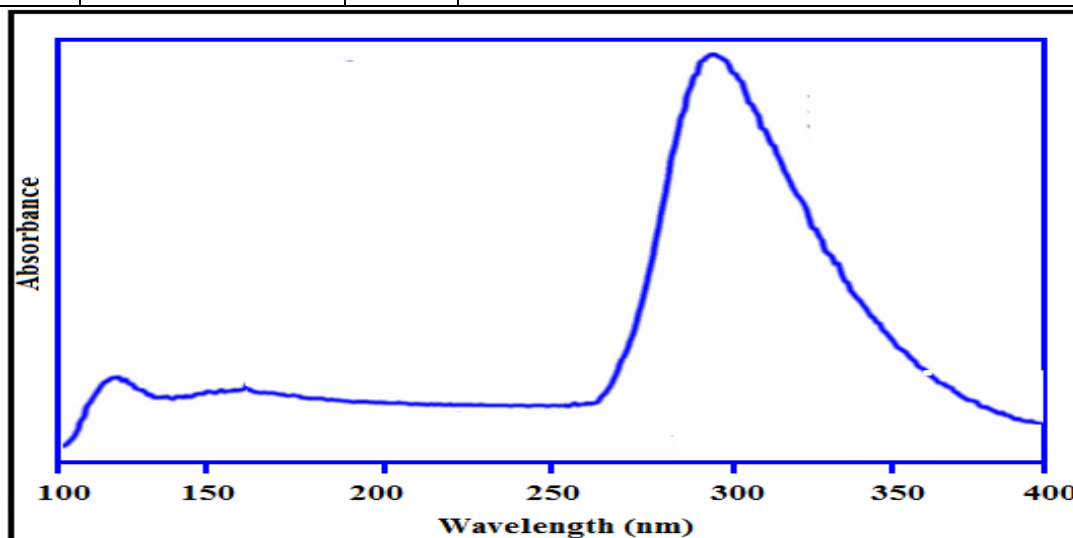| TD-B3LYP/6-311++G(d,p) | | Expt λ_{obs} | Major Contributions |
| Methanol | | | |
λ_{cal}	E (eV)		
320.09	6.219	320	HOMO–>LUMO (83%)
130.34	6.083	120	HOMO–>L+1 (48%)
180.66	6.891	–	H-1–>LUMO (69%), HOMO–>L+1 (31%)

FIGURE 3

UV–VIS SPECTRA OF BEHENIC ACID

MOLECULAR ELECTROSTATIC POTENTIAL SURFACE\

MEP maps are shown in Figure 4. The red color region is a negative charge of the accumulation area with high electron density (ED), while blue color region is positive charge of the gathering area with a lower ED. It is notable that all the negative potentials in these donor/acceptor dyes are distributed on the nitrogen and oxygen

atoms and phenyl rings, while all the positive potentials are distributed on the hydrogen atoms in the C groups. The results clearly indicate that behenic acid in the middle region of the molecule is a rich electron area thus acting as an electron donor, and the itaconimide or maleimide group on both ends of the molecule is a poor electron area serving as an electron acceptor. The isosurface of ED for the molecular is 0.001 electrons per Bohr (Figure 4). The color ranges from −0.0620 and 0.0250 au (red and blue).
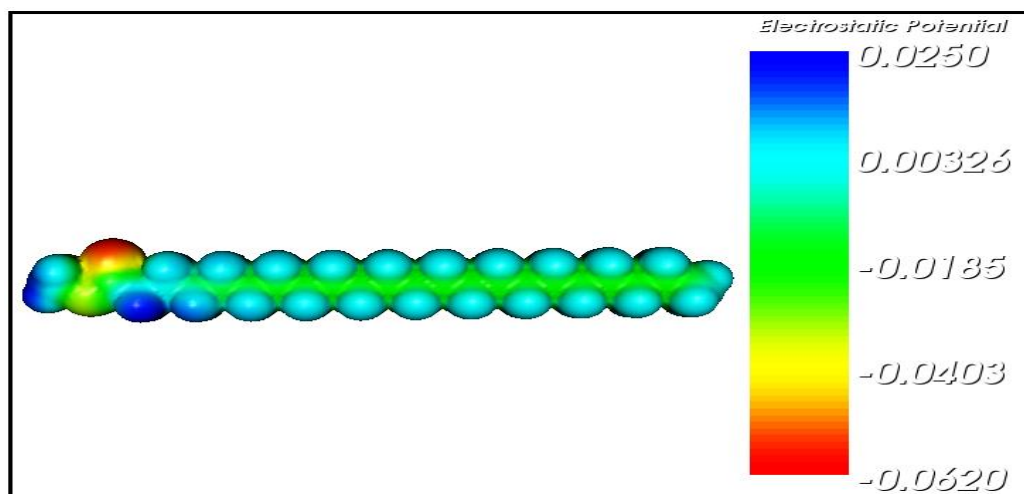

FIGURE 4

MOLECULAR ELECTROSTATIC POTENTIAL OF BEHENIC ACID

NBO ANALYSIS of BEHENIC ACID

Larger the E(2) value, the more intensive is the interaction between electron donors and electron acceptors, i.e., the more donating tendency from electron donors to electron acceptors of the whole system. In this compound, the intramolecular interaction are formed by the orbital overlap between the bonding π C_{25}–H_{70} and the antibonding π^* C_{25}–O_{24} orbital which results in intramolecular charge transfer (ICT) causing stabilization of the system. These interactions are observed as an increase in the ED in the C_{25}–O_{24} antibonding orbital that weakens the respective bond. The most important interaction energies related to the resonance in the molecule is the electron donating from the lone pair LP O_1 atom to LP (2) O_{24} atom to π^* C_1–O_{23} which leads to a stabilization energy of 47.88 KJ/mol as shown in Table IV. Hence the charge transfer interactions explained above are responsible for the pharmaceutical and biological properties [31] of behenic acid.

TABLE IV

NATURAL BOND ORBITAL ANALYSIS OF BEHENIC ACID

Donor NBO (i)	Acceptor NBO (j)	E(2)[a] (kJ/mol)	E(j)–E(i) (a.u.)	F(i,j) (a.u.)
BD (1) C_{25}–H_{70}	BD*(2) C_{25}–O_{24}	5.99	0.49	0.048
LP (2) O_{23}	BD*(1) C_1–C_2	17.26	0.74	0.081
LP (2) O_{23}	BD*(1) C_1–O_{24}	34.30	0.59	0.138
LP (2) O_{24}	BD*(2) C_1–O_{23}	47.88	0.36	0.111

MULLIKEN CHARGE ANALYSIS

In particular, Mulliken and natural charge of all the carbon (C_1) atom carry a negative value in the aliphatic chain lead to a redistribution of ED and most of the carbon atoms hold negative charges except C_1.

TABLE V
MULLIKEN ATOMIC CHARGES OF BEHENIC ACID

Atoms	Mulliken Charge	Atoms	Mulliken Charge
C_1	0.3027	H_{36}	0.0819
C_2	−0.1558	H_{37}	0.0820
C_3	−0.1550	H_{38}	0.0808
C_4	−0.1636	H_{39}	0.0809
C_5	−0.1604	H_{40}	0.0813
C_6	−0.1621	H_{41}	0.0814
C_7	−0.1618	H_{42}	0.0808
C_8	−0.1619	H_{43}	0.0809
C_9	−0.1619	H_{44}	0.0811
C_{10}	−0.1619	H_{45}	0.0811
C_{11}	−0.1619	H_{46}	0.0809
C_{12}	−0.1619	H_{47}	0.0809
C_{13}	−0.1619	H_{48}	0.0810
C_{14}	−0.1619	H_{49}	0.0811
C_{15}	−0.1619	H_{50}	0.0809
C_{16}	−0.1619	H_{51}	0.0809
C_{17}	−0.1619	H_{52}	0.0810
C_{18}	−0.1619	H_{53}	0.0810
C_{19}	−0.1621	H_{54}	0.0809
C_{20}	−0.1617	H_{55}	0.0809
C_{21}	−0.1641	H_{56}	0.0809
C_{22}	−0.2130	H_{57}	0.0810
O_{23}	−0.3600	H_{58}	0.0809
O_{24}	−0.2698	H_{59}	0.0809
C_{25}	−0.0556	H_{60}	0.0808
H_{26}	0.1127	H_{61}	0.0809
H_{27}	0.1128	H_{62}	0.0809
H_{28}	0.0999	H_{63}	0.0810
H_{29}	0.1000	H_{64}	0.0798
H_{30}	0.0806	H_{65}	0.0799
H_{31}	0.0806	H_{66}	0.0718
H_{32}	0.0844	H_{67}	0.0728
H_{33}	0.0845	H_{68}	0.0729
H_{34}	0.0808	H_{69}	0.1052
H_{35}	0.0809	H_{70}	0.0768
		H_{71}	0.0769

The Mulliken and natural charge on H_{27} in the functional group has the maximum magnitude of 0.1128 among the hydrogen atoms present in the compound and here, the entire hydrogen atoms exhibit a net positive charge. But in this charge distribution, it is mainly to note that among repulsion (same charge) and attraction (opposite charge) bonds were appeared. This idea created the loosing bonding and leaving free electrons in the ligand and

thus charge difference were produced. From this observation, it is clear that the molecule was very reactive at functional group side.
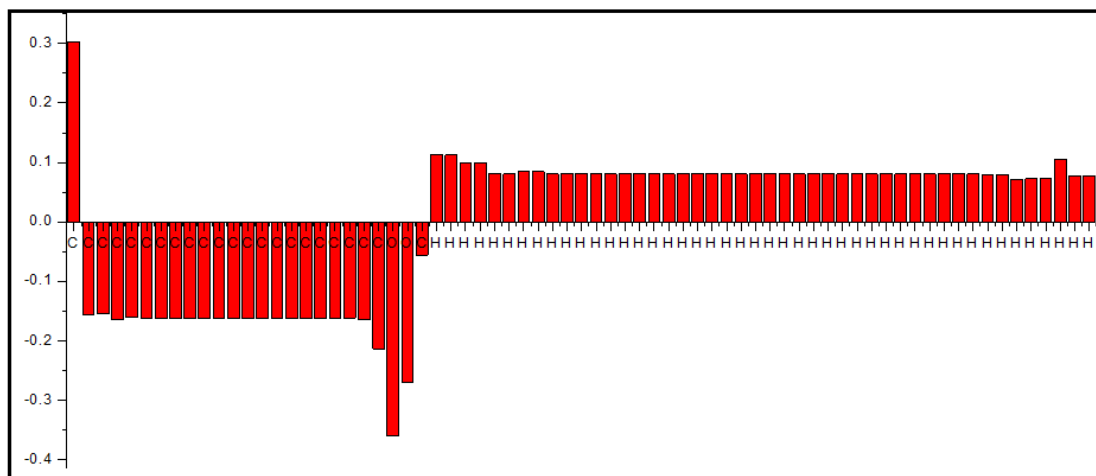

FIGURE 5

MULLIKEN'S ATOMIC CHARGES ANALYSIS OF BEHENIC ACID

CONCLUSION

The present investigation thoroughly analyzed the molecular confirmation of behenic acid using vibrational spectrum and absorption maxima of title compound was calculated by TD-DFT method and compared with experimental UV–Vis spectra. The stability and intramolecular interactions reveals that O_3 and O_4 have the most intensive interaction between the Lewis acceptor and Lewis donor that gives stabilization to the structure. It has been concluded that the lowest singlet excited state of the title molecule is mainly derived from the HOMO/LUMO electron transition. MEP plays an important role in determining stability of the molecule. NBO analysis has been done to find the stability and intermolecular charge transfer between the bonding and antibonding orbital.

REFERENCES

[1]   Shariff, M., Sudarshana, S., Umesha, S., et al., "Antimicrobial activity of Rauvolfia tetraphylla and Physalis minima leaf and callus extracts," African Journal of Biotechnology, Vol. 5, No. 10, 2006, pp. 946–950.

[2]   Vines, G., Herbal Harvests with a Future: Towards Sustainable Sources for Medicinal Plants," Plant Life International, 2004. http://www.plantlife.org.uk/.

[3]   Saet, B.L., Kwang, H.C., Su, N.K., et al., "The antimicrobial activity of essential oil from Dracocephalum foetidum against pathogenic microorganisms," Journal of Microbiology, Vol. 45, No. 1, 2007, pp. 53–57.

[4]   Davis, P.H., Flora of Turkey and East Agean Island, Vol. 7, Edinburg University Press, Edinburg, Tex, USA, 1982.

[5]   Lis-Balchin, M. and Deans, S.G., "Bioactivity of selected plant essential oils against Listeria monocytogenes," Journal of Applied Microbiology, Vol. 82, No. 6, 1997, pp. 759–762.

[6]   Ates, D.A. and Erdogrul, O. T., "Antimicrobial activities of various medicinal and commercial plant extract," Turkish Journal of Biology, Vol. 27, 2003, pp. 157–162.

[7]   El-Seedi, H.R., Ohara, T., Sata, N. et al., "Antimicrobial diterpenoids from *Eupatorium glutinosum* (Asteraceae)," Journal of Ethnopharmacology, Vol. 81, No. 2, 2002, pp. 293–296.

[8] Rojas, B., Bustamante, B., Bauer, J., Fernandez, I., Albán, J. and Lock, O., "Antimicrobial activity of selected Peruvian medicinal plants," Journal of Ethnopharmacology, Vol. 88, No. 2–3, 2003, pp. 199–204.

[9] Duraipandiyan, V., Ayyanar, M. and Ignacimuthu, S., "Antimicrobial activity of some ethnomedicinal plants used by Paliyar tribe from Tamil Nadu, India," BMC Complementary and Alternative Medicine, Vol. 6, 2006, Article 35.

[10] Chemexcil, Selected Medicinal Plants of India, Basic Chemicals, Pharmaceutical and Cosmetic Export Promotion Council, Bombay, India, 1992.

[11] Badam, L., Bedekar, S., Sonawane, K.B. and Joshi, S.P. "In vitro antiviral activity of bael (*Aegle marmelos* Corr.) upon human coxsackieviruses B1–B6," Journal of Communicable Diseases, Vol. 34, No. 2, 2002, pp. 88–99.

[12] Chew, Y.L., Goh, J. K. and Lim, Y.Y., "Assessment of in vitro antioxidant capacity and polyphenolic composition of selected medicinal herbs from Leguminosae family in Peninsular Malaysia," Food Chemistry, Vol. 116, No. 1, 2009, pp. 13–18.

[13] Gupta, A.K. and Tandon, N., Reviews on Indian Medicinal Plants, Vol. 1, Indian Council of Medicinal Research, New Delhi, India, 2004.

[14] Kamalakkannan, N. and Stanely Mainzen Prince, P., "Antihyperlipidaemic effect of *Aegle marmelos* fruit extract in Streptozotocin-induced diabetes in rats," Journal of the Science of Food and Agriculture, Vol. 85, No. 4, 2005, pp. 569–573.

[15] Arul, V., Miyazaki, S. and Dhananjayan, R., "Studies on the anti-inflammatory, antipyretic and analgesic properties of the leaves of *Aegle marmelos* Corr.," Journal of Ethnopharmacology, Vol. 96, No. 1–2, 2005, pp. 159–163.

[16] Jagetia, G.C., Venkatesh, P. and Baliga, M.S., "*Aegle marmelos* (L.) Correa inhibits the proliferation of transplanted Ehrlich ascites carcinoma in mice," Biological and Pharmaceutical Bulletin, Vol. 28, No. 1, 2005, pp. 58–64.

[17] Kamalakkannan, N. and Prince, P.S.M., "Hypoglycaemic effect of water extracts of *Aegle marmelos* fruits in Streptozotocin diabetic rats," Journal of Ethnopharmacology, Vol. 87, No. 2–3, pp. 207–210, 2003.

[18] Rajadurai, M., Padmanabhan, M. and Prince, P.S.M., "Effect of *Aegle marmelos* leaf extract and alpha-tocopherol on lipid peroxidation and antioxidants in isoproterenol-induced myocardial infarction in rats," Cardiology, Vol. 1, 2005, pp. 40–45.

[19] Sabu, M.C., Kuttan, R., Antidiabetic activity of *Aegle marmelos* and its relationship with its antioxident properties. Indian Journal of Pharmacology, Vol. 48, 2004, pp. 81–88.

[20] Saradha Jyothi, K. and Subba Rao, B., "Antibacterial activity of extracts from *Aegle marmelos* against standard pathogenic bacterial strains," International Journal of PharmTech Research, Vol. 2, No. 3, 2010, pp. 1824–1826.

[21] Sur, T.K., Pandit, S. and Pramanik, T., "Antispermatogenic activity of leaves of *Aegle marmelos* corr. in albino rats: a preliminary report," Biomedicine, Vol. 19, No. 3, 1999, pp. 199–202.

[22] Yen, G.C., Duh, P.D. and Tsai, C.L., "Relationship between antioxidant activity and maturity of peanut hulls," Journal of Agricultural and Food Chemistry, Vol. 41, No. 5, 1993, pp. 67–70.

[23] Kingston, C., Jeeva, S., Jeeva, G.M., et al., "Indigenous knowledge of using medicinal plants in treating skin diseases in Kanyakumari District, Southern India," Indian Journal of Traditional Knowledge, Vol. 8, No. 2, 2009, pp. 196– 2009.

[24] Cowan, M.M, "Plant products as antimicrobial agents," Clinical Microbiology Reviews, Vol. 12, No. 4, 1999, pp. 564–582.

[25] Frisch, M.J., Trucks, G.W. and Schlegel, H.B., et al., Gaussion 09W, Revision A.02, GaussionInc, Walling ford, CT, 2009.

[26] Krishnakumar, V., Surumbarkuzhali, N. and Muthunatesan, S., Spectrochimica Acta, Part A: Molecular and Biomolecular Spectroscopy, Vol. 71, 2009, p. 1810.

[27] Bardakçı, T. and Kumru, M., "Molecular structure, vibrational and EPR spectra of Cu(II) chloride complex of 4-amino-1-methylbenzene combined with quantum chemical calculations," Journal of Molecular Structure, Vol. 1054–1055, 2013, pp. 76–82.

[28] Prabakaran, A.R. and Mohan, S., Indian Journal of Physics, Vol., 63B, 1989, p. 468.

[29] Kumru, M., Küçük, V., Kocademir, M., et al. "Experimental and theoretical studies on IR, Raman, and UV–Vis spectra of quinoline-7-carboxaldehyde," Spectrochimica Acta Part A: Molecular and Biomolecular Spectroscopy, Vol. 134, 2015, pp. 81–89.

[30] Aloysius, A., Ramanathan, R., Christy, A., et al., "Experimental and theoretical studies on the corrosion inhibition of vitamins – thiamine hydrochloride or biotin in corrosion of mild steel in aqueous chloride environment," Egyptian Journal of Petroleum, Vol. 27, 2018, pp. 371–381.

[31] Uppal, A., Kamni and Khajuria, Y., "Spectroscopic, thermodynamic properties and Fukui function analysis of (4Z)-2-phenyl-1-{(E)-[4-propan-2-yl)benzylidene]amino}-4-[(thiophen-2-yl)methylidene]-1 H-imidazol 5(4H)-one}," Journal of Molecular Structure, Vol. 1179, 2019, pp. 1–820.